CYTOMETRY
Journal of Quantitative Cell Science PART A

Titrating Complex Mass Cytometry Panels

Stein-Erik Gullaksen,[1] Lucius Bader,[2,3] Monica Hellesøy,[4] André Sulen,[1] Oda Helen Eck Fagerholt,[1] Caroline B. Engen,[1] Jørn Skavland,[1] Bjørn Tore Gjertsen,[1,4] Sonia Gavasso[5,6*]

[1]Centre of Cancer Biomarkers CCBIO, Department of Clinical Science, University of Bergen, Bergen, Norway

[2]Department of Clinical Science, University of Bergen, Bergen, Norway

[3]Bergen group of Epidemiology and Biomarkers in Rheumatic Disease (BEaBIRD), Department of Rheumatology, Haukeland University Hospital, Bergen, Norway

[4]Department of Internal Medicine, Hematology section, Helse Bergen, Bergen, Norway

[5]Department of Clinical Medicine, University of Bergen, Bergen, Norway

[6]Neuroimmunology Lab, Haukeland University Hospital, Bergen, Norway

Received 23 August 2018; Revised 26 February 2019; Accepted 28 February 2019

Grant sponsor: The Research Council of Norway, Grant number: 220759; Grant sponsor: Helse Vest health Trust, Project numbers: 912160, 912009; Grant sponsor: Norwegian Cancer Society Legacy, Grant numbers: 104712, 145268, 145269 and 163424

Additional Supporting Information may be found in the online version of this article.

*Correspondence to: Sonia Gavasso, Department of Neurology, Haukeland University Hospital, Jonas Lies Vei 65, 5021 Bergen, Norway. Email: sonia.gavasso@helse-bergen.no

Published online 9 April 2019 in Wiley Online Library (wileyonlinelibrary.com)

DOI: 10.1002/cyto.a.23751

Abstract

We describe here a simple and efficient antibody titration approach for cell-surface markers and intracellular cell signaling targets for mass cytometry. The iterative approach builds upon a well-characterized backbone panel of antibodies and analysis using bioinformatic tools such as SPADE. Healthy peripheral blood and bone marrow cells are stained with a pre-optimized "backbone" antibody panel in addition to the progressively diluted (titrated) antibodies. Clustering based on the backbone panel enables the titration of each antibody against a rich hematopoietic background and assures that nonspecific binding and signal spillover can be quantified accurately. Using a slightly expanded backbone panel, antibodies quantifying changes in transcription factors and phosphorylated antigens are titrated on *ex vivo* stimulated cells to optimize sensitivity and evaluate baseline expression. Based on this information, complex panels of antibodies can be thoroughly optimized for use on healthy whole blood and bone marrow and are easily adaptable to the investigation of samples from for example clinical studies. © 2019 The Authors. *Cytometry Part A* published by Wiley Periodicals, Inc. on behalf of International Society for Advancement of Cytometry.

Key terms

mass cytometry; panel design; antibody titration; whole blood; bone marrow; CyTOF; phosphoflow

MASS cytometry enables the simultaneous measurement of over 40 antigens on single cells using metal isotope conjugated antibodies, generating highly complex datasets with minimal experimental artifacts (1–3). As the number of antibodies used to investigate biologically heterogeneous cells increases, so do the demands for an efficient and thorough approach to determine optimal antibody titers. In addition to undesirable signal arising from nonspecific antibody binding, which is an issue in all types of antibody-based assays, three sources of signal spillover exist in mass cytometry (4,5): signal overlap of highly abundant metal isotopes into adjacent mass channels (±1 Da), isotope oxidation (+16 Da), and isotopic impurities in the metal isotopes. Although technical approaches to deal with similar experimental artifacts have been well established for conventional flow cytometry (6), mass cytometry has unique requirements (7).

The predictable patterns of signal spillover in mass cytometry are not routinely compensated, as is commonplace in conventional flow cytometry. Although such compensation tools have been developed (8), signal spillover can be significantly reduced by lowering the signal intensities (linearly dependent) and/or by carefully designing antibody panels (9). The former may not allow for sufficient distance between the biologically positive and dim/negative populations, and the latter may introduce unwanted/unnecessary noise in the data. In contrast to conventional flow cytometry the range of "brightness" observed across the mass range of purified metal isotope tags is fairly equal (1,10). Thus, the choice of isotope may not always provide

the staining characteristics needed to capture the biological diversity within the mass cytometers dynamic range, without accepting signal spillover to some degree. Antibody binding to secondary and low affinity epitopes must also be evaluated. This might be a challenging process as the combinatorial possibilities of marker expression quickly exceeds our understanding of the human immune system with increasing numbers of markers. Lastly, we emphasize that determination of optimized antibody titer is application-specific and is not necessarily transferrable between different biological samples, processing protocols, laboratories, or antibody lots. In addition, we have also observed a variation in the stability of metal conjugated antibodies, potentially changing the optimal titer over time. Taken together, the construction of large antibody panels for mass cytometry is an extremely time consuming, laborious, and demanding undertaking, necessitating an efficient and straightforward approach.

Materials and Methods

Subjects and Samples

Peripheral blood (PB) and Bone marrow (BM) samples were obtained from healthy individuals who provided written informed consent (local ethical committee approval 2012/2247). PB and BM were collected in the presence of heparin. The leukocytes were fixed and erythrocytes lysed using Lyse/Fix buffer (BD Biosciences) within 1 h, and samples were stored at −80°C in physiological saline.

Ex Vivo Stimulation of Peripheral Blood and Bone Marrow

Freshly collected PB and BM from one healthy donor were stimulated *ex vivo* with IFN-α (100 ng/ml, 15 min), GM-CSF (100 ng/ml, 15 min), LPS (10 μg/ml, 15 min), or left untreated. PB and BM cells were fixed, and erythrocytes lysed using the BD Lyse/Fix reagent as above.

Barcoding and Antibody Staining

Fixed leukocytes from PB and BM were barcoded (3) using the Fluidigm 20-plex metal barcoding kit according to manufacturer's protocol. All antibodies used in this study were either purchased pre-conjugated from Fluidigm or were conjugated in-house using the X8 MaxPar conjugation kits according to manufacturer's protocol (Online Tables 1–3). See the online materials for detailed protocols. Briefly, aliquots of 1.5×10^6 cells were first pretreated with heparin (100 IU/ml, 20 min) (11) and then stained with mastermixes of backbone antibody panel mixed with twofold serially diluted panel of antibodies to be titrated in a total staining volume of 50 μl (30 min, room temperature). The dilution of most antibodies started at the concentration recommended by the manufacturer (1 μl antibody per 100 μl cell suspension containing 3×10^6 cells). However, for some antibodies, a pre-dilution was necessary before a twofold titration was possible. For instance, the ^{163}Dy-CD56 was diluted by a factor of 10× (Online Fig. 8) before the twofold dilution shown in Supplemental Figure 2. Cells to be stained with intracellular signal transduction antibodies were permeabilized for 10 min on ice with methanol (−20°C, 100%), treated with heparin (100 IU/ml, 20 min) and subsequently stained with progressively titrated (five twofold dilutions) intracellular antibodies (30 min, room temperature). To enable the identification of cells, the DNA was labeled with iridium-191/193 by incubation in 0.1 nM Ir-nucleic acid intercalator (Fluidigm) diluted in MaxPar PBS containing 4% PFA (Alfa Aesar, 16% PFA, methanol-free) overnight at 4°C. Cells that were not permeabilized with methanol (cell surface only) were labeled with iridium-191/193 by incubating with Ir-nucleic acid intercalator (0.1 nM) diluted in MaxPar Fix/perm buffer (Fluidigm) overnight at 4°C. Immediately before sample acquisition, cells were washed in MaxPar cell staining buffer and MaxPar water (both from Fluidigm) and left pelleted until analysis on the Helios mass cytometer (Fluidigm). The cells were resuspended in MaxPar water supplemented with a 1:10 dilution of the EQ Four Element calibration beads (Fluidigm). The acquisition rate was kept below 400 cells per second to limit the number of acquired cell doublets.

Data Analysis

Machine drift in the data was normalized using the Fluidigm bead normalizer. Cell debris and doublets were manually removed by gating on event length and DNA (Ir-191/193). The Fluidigm barcode de-convolution tool was used for de-barcoding samples. The histogram overlay illustrations were made, and SPADE (12) analysis was performed, in cytobank.org. Sample concatenation and gating was performed in FlowJo (FLOWJO, LLC). For gated populations, the 75th percentile of the dual count in each mass channel was exported for statistics. The heat maps were made using Morpheus (https://software.broadinstitute.org/morpheus/).

Results and Discussion

A graphical illustration of our approach is presented in Figure 1, and a more detailed description is given in the Online Materials. All reagents used in this work can be found in Online Tables 1–3. A backbone panel (Online Table 4) of carefully selected antibodies was established as basis to evaluate the titration of additional antibodies in titration step 1. Titration data for the backbone panel is shown in Figure 1a and Online Figure 1a. The optimal titer for each antibody (red gate) was approximated by contrasting the ability to securely discern positive from negative cells against signal spillover into other mass channels. For example, low-level spillover of 2–3 dual counts of ^{145}Nd-CD4 signal into ^{146}Nd-CD8 can be accepted, as long as co-expression of CD8 is not of biologic interest. In titration step 2, after optimization of the backbone panel, sample aliquots of metal barcoded (3) and paired PB and BM from two healthy donors were stained with the backbone panel and serially diluted mastermixes of the three "titration panels" (Online Table 6) containing additional cell surface antibodies (Fig. 1b). In these titration panels, all channels theoretically receiving spillover from the included markers were kept empty. For example, ^{144}Nd-CD38 and ^{148}Nd-CD16 were placed in different titration panels. We used the SPADE

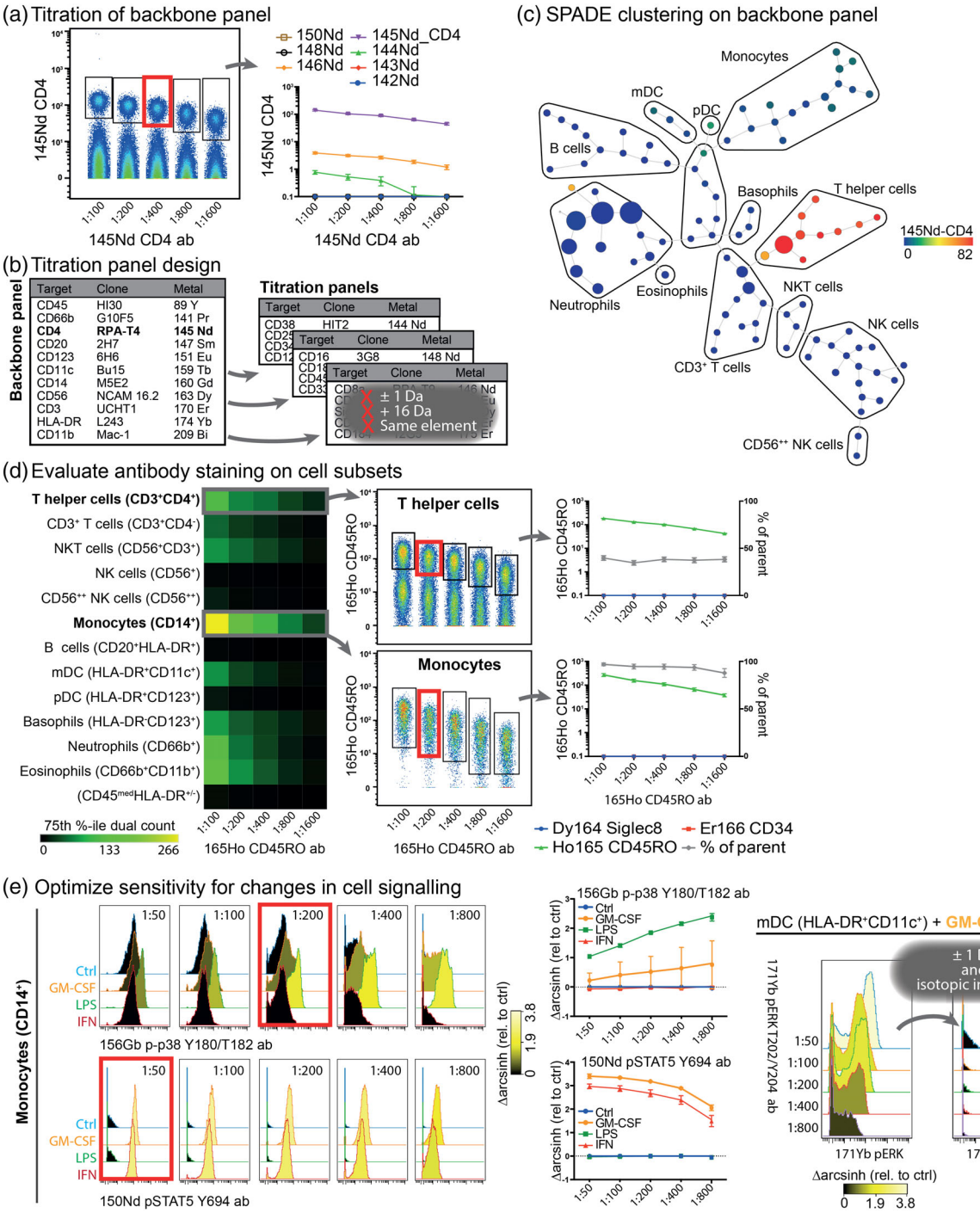

Figure 1. (a) A backbone panel was titrated using PB and BM from two healthy donors. The .fcs files were concatenated to visualize immune staining as a function of antibody concentration and to enable efficient gating of positive cells. The expression of the titrated antigen and all spillovers (±1 Da, +16 Da and channels detecting isotopic impurities) was calculated for the gated cells plotted (75th %-ile dual counts). Optimal titer (red gate) was chosen by balancing the ability to discern positive from negative cells with the amount of signal overlap generated in other mass channels. (b) Additional cell surface antibodies to be titrated were subdivided into titration panels. Here, all channels receiving spillover were unused in each panel. Cell sample aliquots were stained with the titrated backbone panel and serially diluted mastermixes of the titration panels. (c) A single SPADE clustering was performed to efficiently identify cell subsets in the entire data set. The clustering was based solely on the backbone panel, and cell subsets manually identified. (d) The signal from the titrated antibodies were measured in each of the cell subsets and plotted as a heat map. The data was in selected cell subsets concatenated, and the expression of the titrated antigen and all spillovers calculated for the gated population, as above. The exact staining pattern on a relevant cell subset (i.e., CD45RO expression on T helper cells) could now also be evaluated in addition to signal spillover (i.e., CD45RO expression on monocytes) and panel design. The red gate indicates the chosen antibody titer. The relative abundance of positive cells in the parent cell subset as a function of antibody concentration was also calculated. (e) PB and BM from one healthy donor were stimulated ex vivo with GM-CSF (100 ng/ml, 15 min), IFN-α (100 ng/ml, 15 min) or LPS (10 μg/ml, 15 min) or left untreated. The antibodies to be titrated were split into two titration panels, as above. Cells were stained with backbone panel and serially diluted titration panels, and cell subsets identified using SPADE. The phosphorylation level (75th %-ile) was measured in each population, for all intracellular antibodies and all channels theoretically receiving spillover. Drug-induced changes in phosphorylation levels were calculated (Δarcsinh relative to ctrl) and plotted as a function of antibody dilution. Lastly, the signal spillover generated by induction of signaling into the empty mass channel was evaluated. Red boxes indicate optimal dilutions of antibodies. Color scales indicate Δarcsinh relative to control.

Table 1. Antibody panel. (See online Tables 1–4, 6, and 8 in the online materials for more details)

SPECIFICITY	CLONE	ISOTOPE	PURPOSE
CD45	HI30	89 Y	Pan leukocytes
CD66b	G10F5	141 Pr	Neutrophils
Cleaved caspase 3	D3E9	142 Nd	Apoptosis
CD38	HIT2	144 Nd	Activation
CD4	RPA-T4	145 Nd	T helper cells
CD8a	RPA-T8	146 Nd	Cytotoxic T cells
CD20	2H7	147 Sm	B cells
CD16	3G8	148 Nd	Neutrophils and subsets of NK and monocytes
CD25	2A3	149 Sm	Basophils, Tregs, and activated T helper cells
pSTAT5 Y694	47	150 Nd	Signal transduction
CD123	6H6	151 Eu	Basophils, mDC, and pDC
pSTAT1 Y701	58D6	153 Eu	Signal transduction
p-p38 T180/Y182	D3F9	156 Gd	Signal transduction
pSTAT3 Y705	4/P-STAT3	158 Gd	Signal transduction
CD11c	Bu15	159 Tb	Monocytes and mDC
CD14	M5E2	160 Gd	Monocytes
CD181 (IL-8RA)	B1	161 Dy	Neutrophils
FoxP3	PCH101	162 Dy	Tregs
CD56	NCAM 16.2	163 Dy	NK cells
CD45RO	UCHL1	165 Ho	Naïve/memory T cells
CD34	581	166 Er	Hematopoietic stem/progenitor cell
CD1c (BDCA-1)	L161	167 Er	Subsets of mDC and B cells
CD335 (NKp46)	9E2	169 Tm	NK cells
CD3	UCHT1	170 Er	T cells
pERK 1/2 T202/Y204	D1314.E4	171 Yb	Signal transduction
HLA-DR	L243	174 Yb	Activation, DCs, monocytes, and B cells
CD184 (CXCR4)	12G5	175 Lu	Basophils
pCREB S133	87G3	176 Yb	Signal transduction
CD11b	Mac-1	209 Bi	Granulocytes, monocytes NK cells, and DCs

mDC; myeloid dendritic cell; pDC, plasmacytoid dendritic cell; NK, natural killer; Tregs, regulatory T cells.

clustering algorithm (12) in Cytobank.org to identify common cell subsets across all files in the experiment based on backbone antigen expression (Fig. 1c and Online Fig. 2). This clustering provided a rich immune-phenotypic background on which the titration of the additional antibodies could be evaluated (Fig. 1d and Online Fig. 1b–d). In addition to evaluating signal spillover using the cell population with the highest expression (e.g., CD45RO on monocytes) as in step 1, this also allowed for the exact evaluation of the staining pattern in a biologically relevant cell subset (e.g., T helper cells). In this way, staining characteristics can be seen across a wider hematological background, altogether further refining the approximation of optimal titers (indicated in red boxes). In titration step 3, we evaluated antibodies specific for intracellular cell signaling and transcription factors. A metal barcoded pool of *ex vivo* stimulated PB and BM (IFN-α [100 ng/ml, 15 min], GM-CSF [100 ng/ml, 15 min], LPS [10 μg/ml, 15 min]) was stained with a combined backbone panel based on titration steps 1 and 2, and progressively diluted titration panels as described above (Online Table 8). After SPADE clustering on surface antigen expression as above (Online Figs. 3 and 4), we calculated the stimulation-induced change in cell signaling (Δarcsinh relative to control) for all cell subsets (Fig. 1e and Online Fig. 5). Of note, in our experiment the Δarcsinh after both GM-CSF and LPS stimulation increased for p-p38 Y180/T182 in monocytes ($CD14^+$) with increasing dilution of the antibody. Likely, surplus antibody created an increased background, thus masking a drug-induced regulation in signal transduction after stimulation. This emphasizes the importance of selecting optimal antibody titers using appropriate biological controls. Furthermore, we assessed the signal spillover as a function of drug-induced alterations in cell signaling. For example, after GM-CSF stimulation, we could measure spillover signal into the empty ^{172}Yb channel induced by high phosphorylation levels of pERK1/2 Y202/T204 (^{171}Yb) in the myeloid dendritic cell population (mDCs, $CD11c^+HLA\text{-}DR^+$). This spillover decreased as a function of antibody titration (Fig. 1e, right panel). The final choice of antibody titers was done by minimizing signal spillover and optimal resolution between positive/stimulated and negative/baseline. We validated our approach by testing the titrated panel (Table 1 and Online Table 1 and 2) on three additional healthy donor PB samples. The staining patterns of both cell surface markers and intracellular signal transduction targets in these additional samples reproduced the antibody

titration results, highlighting the usefulness of our approach (See online materials and Online Figs. 6 and 7).

In summary, we outline here a conceptual framework where we highlight the usefulness of performing iterative antibody titration on cells stained with a backbone panel. We found SPADE to be an excellent tool for automated cell clustering based on the backbone panel. SPADE enabled clustering of cells in a dataset consisting of more than 6 million cells into a single SPADE tree. Using bioinformatic tools, this approach is efficient and straightforward and provides a deeper characterization of each antibody's performance, which is necessary for the demanding task of panel design for mass cytometry assays. Although we have demonstrated the titration of antibodies on healthy PB and BM in this work, this approach can easily be adapted to other sample types for mass cytometry.

Acknowledgments

This study was supported by The Research Council of Norway (Petromaks program grant #220759), Helse Vest Health Trust (project no. 912160, 912009), and the Norwegian Cancer Society Legacy (Grant no. 104712, 145268, 145269 and 163424) with Solveig & Ole Lunds Legacy. The Helios mass cytometry instrument was a generous gift from the Trond Mohn Foundation.

Literature Cited

1. Spitzer MH, Nolan GP. Mass cytometry: Single cells, many features. Cell 2016;165(4):780–791.
2. Catena R, Ozcan A, Zivanovic N, Bodenmiller B. Enhanced multiplexing in mass cytometry using osmium and ruthenium tetroxide species. Cytometry A 2016;89(5):491–497.
3. Zunder ER, Finck R, Behbehani GK, Amir el AD, Krishnaswamy S, Gonzalez VD, et al. Palladium-based mass tag cell barcoding with a doublet-filtering scheme and single-cell deconvolution algorithm. Nat Protoc 2015;10(2):316–333.
4. Ornatsky OI, Kinach R, Bandura DR, Lou X, Tanner SD, Baranov VI, Nitz M, Winnik MA. Development of analytical methods for multiplex bio-assay with inductively coupled plasma mass spectrometry. J Anal At Spectrom 2008;23(4):463–469.
5. Bendall SC, Nolan GP, Roederer M, Chattopadhyay PK. A deep profiler's guide to cytometry. Trends Immunol 2012;33(7):323–332.
6. Mahnke YD, Roederer M. Optimizing a multicolor immunophenotyping assay. Clin Lab Med 2007;27(3):469–485.
7. Takahashi C, Au-Yeung A, Fuh F, Ramirez-Montagut T, Bolen C, Mathews W, O'Gorman WE. Mass cytometry panel optimization through the designed distribution of signal interference. Cytometry A 2017;91(1):39–47.
8. Chevrier S, Crowell HL, Zanotelli VRT, Engler S, Robinson MD, Bodenmiller B. Compensation of signal spillover in suspension and imaging mass cytometry. Cell Syst 2018;6(5):612–620.
9. Leipold MD, Newell EW, Maecker HT. Multiparameter phenotyping of human PBMCs using mass cytometry. Methods Mol Biol 2015;1(343):81–95.
10. Tricot S, Meyrand M, Sammicheli C, Elhmouzi-Younes J, Corneau A, Bertholet S, Malissen M, le Grand R, Nuti S, Luche H, et al. Evaluating the efficiency of isotope transmission for improved panel design and a comparison of the detection sensitivities of mass cytometer instruments. Cytometry A 2015;87(4):357–368.
11. Rahman AH, Tordesillas L, Berin MC. Heparin reduces nonspecific eosinophil staining artifacts in mass cytometry experiments. Cytometry Part A 2016;89(6):601–607.
12. Qiu P, Simonds EF, Bendall SC, Gibbs KD Jr, Bruggner RV, Linderman MD, et al. Extracting a cellular hierarchy from high-dimensional cytometry data with SPADE. Nat Biotechnol 2011;29(10):886–891.